LAWRENCE
LIVERMORE
NATIONAL
LABORATORY

Nonlinear pulse combining and pulse compression in multi-core fibers

A. M. Rubenchik, L. S. Chekhovskoy, M. P. Fedoruk, O. V. Shtyrina, S. K. Turitsyn

November 24, 2014

Disclaimer

This document was prepared as an account of work sponsored by an agency of the United States government. Neither the United States government nor Lawrence Livermore National Security, LLC, nor any of their employees makes any warranty, expressed or implied, or assumes any legal liability or responsibility for the accuracy, completeness, or usefulness of any information, apparatus, product, or process disclosed, or represents that its use would not infringe privately owned rights. Reference herein to any specific commercial product, process, or service by trade name, trademark, manufacturer, or otherwise does not necessarily constitute or imply its endorsement, recommendation, or favoring by the United States government or Lawrence Livermore National Security, LLC. The views and opinions of authors expressed herein do not necessarily state or reflect those of the United States government or Lawrence Livermore National Security, LLC, and shall not be used for advertising or product endorsement purposes.

Nonlinear pulse combining and pulse compression in multi-core fibers

A. M. Rubenchik,[1] **I. S. Chekhovskoy,**[2,3] **M. P. Fedoruk,**[2,3] **O. V. Shtyrina,**[2,3] **and S. K. Turitsyn**[2,4]

[1]*Lawrence Livermore National Laboratory, Livermore, California 94550, USA*
[2]*Novosibirsk State University, Novosibirsk 630090, Russia*
[3]*Institute for Computational Technologies, SB RAS, Novosibirsk 630090, Russia*
[4]*Aston Institute of Photonic Technologies, Aston University, Birmingham B4 7ET, UK*

We demonstrate the light pulse combining and pulse compression using a continuous-discrete nonlinear system implemented in multi-core fiber (MCF). It is shown that the pulses initially injected into all cores of a ring MCF are combined by nonlinearity into a few cores with simultaneous pulse compression. In 20-core MCF we demonstrate combining of 77% of energy into one core with pulse compressions over 14x. We also demonstrate a suggested scheme that is unsensitive to the phase perturbations. Nonlinear spatio-temporal pulse manipulation in multi-core fibers can be exploited for various applications including pulse compression, switching and combining. © 2014 Optical Society of America

OCIS codes: (190.4360) Nonlinear optics, devices; (060.4370) Nonlinear optics, fibers.

Optical multi-core fibers (MCFs) have recently attracted a great deal of attention in the context of spatial-division multiplexing for high capacity optical communications (see e.g. [1,2] and references therein). In conventional optical communications the nonlinear effects that occur during signal propagation in a fiber are somewhat undesirable.

However, at high signal power, developed MCFs can be also considered as nonlinear discrete physical system, interesting for both fundamental science [3,4] and for practical applications as a nonlinear photonic devices [5–7]. In particular, nonlinear induced collapse (self-focusing, blow-up) of the initial wave packet can be used for pulse compression [8]. The theoretical background for such an approach in the case of non-linear discrete optical arrays has been developed in [6,7]. It has been shown in [6,7] that wave collapse leads to the localization of energy in a small number of cores with simultaneous amplification and compression.

The nonlinear dynamics in MCFs has an interesting link with the light bullets (LBs) proposed in [9]. The light bullets in waveguide arrays have been recently demonstrated and studied in [10,11]. The light bullets studied in [10,11] are discrete optical spatio-temporal solitons. Discrete-continuous system such as the MCFs may prevent the wave collapse, typical for light dynamics in multi-dimensional continuous non-linear medium [12,13]. In this Letter, we demonstrate that nonlinear energy localisation in MCFs may be used for pulse combining and compression. We consider the optical MCFs with circular ring symmetry of their cores shown in Figure 1. Note that many of the obtained results are generic and are applicable to various other MCF configurations.

The propagation of light down MCFs can be approximately (neglecting polarisation characteristics for the sake of clarity) described as a superposition of modes localised at each core:

$$E(x,y,z,t) = \sum_k A_k(z,t)F_k(x-x_k, y-y_k)e^{i(\beta_k z - \omega t)} + cc, \quad (1)$$

where F_k is the spatial mode structure and A_k is the envelope of the electromagnetic field in k-th core. In the limit of a weak coupling approximation one can derive a system of equations for the envelopes A_k, i.e., the continuous-discrete nonlinear Schrodinger equation [14]:

$$i\frac{\partial A_k}{\partial z} = \frac{\beta_2^k}{2}\frac{\partial^2 A_k}{\partial t^2} - \gamma_k|A_k|^2 A_k - \sum_{m=1}^{N} C_{km}A_m, \quad (2)$$

here $k = 1,...,N$, β_2^k is the group-velocity dispersion parameter for the mode k, γ_k is the Kerr parameter, and the C_{km} are the coupling coefficients between the cores.

System (2) can be simplified for the identical cores as discussed in [6,7]. Taking into account the most important physical effects we can simplify the analysis with the following assumption

$$C_{kk} = C_1 > 0, \ C_{k,k+1} = C > 0 \quad (3)$$

and neglect all other coupling terms. To for sake of clarity we consider in what follows $\beta_2^k = \beta_2$, $\gamma_k = \gamma$ ($k = 1,...,N$), however, results can be easily extended to more general cases.

It is convenient to introduce normalized variables: $A_k = \sqrt{\frac{C}{\gamma}}U_k e^{i(2+C_1/C)z'}$, where $z' = z/L$, $L = 1/C$, $t' = t/T$, $T^2 = -\beta_2/(2C)$. The dimensionless equations (omitting the primes) read:

$$i\frac{\partial U_k}{\partial z} = -\frac{\partial^2 U_k}{\partial t^2} - (U_{k+1} - 2U_k + U_{k-1}) - |U_k|^2 U_k. \quad (4)$$

The system (4) is the Hamiltonian one

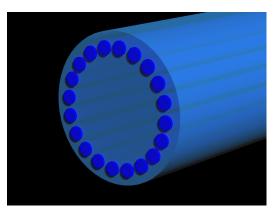$$i\frac{\partial U_k}{\partial z} = \frac{\delta H}{\delta U_k^*} \quad (5)$$

1

Figure 1. Schematic depiction of considered multi-core fiber – waveguide with cores arranged in a circle.

with

$$H = \sum_{k=1}^{N} \int_{-\infty}^{\infty} \left[\left| \frac{\partial U_k}{\partial t} \right|^2 + |U_k - U_{k-1}|^2 - \frac{|U_k|^4}{2} \right] dt. \quad (6)$$

The system (4) conserves H and total power (normalized by C/γ)

$$P_t = \sum_{k=1}^{N} \int_{-\infty}^{\infty} |U_k(z,t)|^2 dt. \quad (7)$$

To understand qualitatively the evolution of pulses injected into an MCF consider first a system with large N and smooth intensity distribution, having only small changes between neighboring cores. In this case we can derive the continuous version of (4) for $U(k,t,z)$

$$i\frac{\partial U}{\partial z} + \frac{\partial^2 U}{\partial t^2} + \frac{\partial^2 U}{\partial k^2} + |U|^2 U = 0, \quad (8)$$

$$H = \int_{-\infty}^{\infty} \left[\left| \frac{\partial U}{\partial t} \right|^2 + \left| \frac{\partial U}{\partial k} \right| - \frac{|U|^4}{2} \right] dt. \quad (9)$$

The eq. (8) is equivalent to the nonlinear Schroedinger equation (NLSE) describing the self-focusing of light in a nonlinear media. If the power at the entrance to the MCF exceeds the critical value $P_{cr} = 11.69$, making $H < 0$, the intensity distribution is self-compressed over k and t. We can expect that the injected MCF pulses distributed over the cores with smooth maxima will be focused into a few cores around the maxima with simultaneous pulse compression. When the energy is concentrated into a few cores the discreteness of the cores arrests further compression.

This scenario has been verified via numerical experiments. In our modelling we have used the same Gaussian pulses in each core, but slightly perturbed the amplitudes from core to core to initiate an instability:

$$U_k = \sqrt{P} \exp\left(-\frac{t^2}{2\tau^2} \right) \left[1 + 0.03 \cos\left(\frac{2\pi k}{N} \right) \right]. \quad (10)$$

The corresponding distribution of total power P_t over the cores is symmetrical with respect to the Nth core and
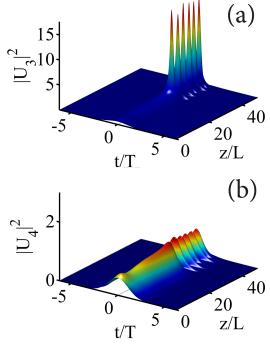

Figure 2. The evolution of input Gaussian pulses (10) with parameters $P = 0.61$, $\tau = 1.5$ is shown for the third core where most of energy is concentrated after propagation. Also shown is the fourth core as an example of dynamics in a neighboring cores of the 6-core fiber. Note the different power scales for the third and fourth cores.

has one maximum at $k = N$, with symmetry between $k = l$ and $k = N - l$. As a result, below we will plot the information for only half of cores. In the numerical computations we used the split-step Fourier method with the Pade approximation with scaling and squaring for matrix exponent (see [15], [16]).

To have compression of the input light distribution as a whole, it is necessary to have at the input $U \sim \sqrt{P} \sim 2/N \sim 1/\tau$. We used this simple guide rule to determine our choice of the initial pulse width and energy.

As can be seen from (10), the pulse amplitudes are perturbed by no more than 3%. The increase of the initial modulation (if it is still small) does not effect the qualitative behaviour, but does accelerate the process development.

The evolution of Gaussian pulses (10) for $N = 6$ is presented on the Fig.2. One can see the combining of almost all of the injected energy into one of the pulses with simultaneous pulse compression. For the specific case presented in Fig.2 with parameters $P = 0.61$, $\tau = 1.5$ we observed the peak power increase to be 30.6x, with pulse duration compressions of 6.6x. The maximum compression is reached at $z = z_0 = 33.3$. One can see that at $z_0 = 33.3$, $\sim 82.8\%$ of the initial energy is concentrated into a single core. Further propagation leads to periodic oscillations of the light intensity. This is the result of the conservation of the Hamiltonian H, that is in general different at the input from the asymptotic value at steady state. Therefore, part of the energy should go into oscil-
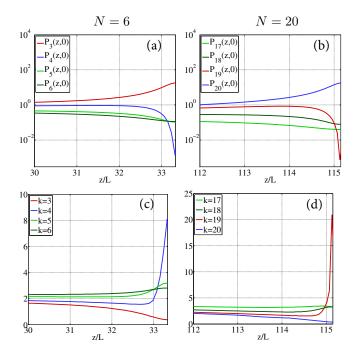
Figure 3. (a) The dynamic of the peak powers (upper pictures) and pulse widths (bottom pictures) of input Gaussian pulses (10) with parameters $P = 0.61$, $\tau = 1.5$ in 3–6-th cores of 6-core MCF (a and c) and pulses with parameters $P = 0.08035$, $\tau = 3.85$ in 17–20 cores for 20-core MCF (b and d). Graphs (c) and (d) show the dynamics of full width at half maximum (FWHM) of corresponding pulses.

Figure 4. The temporal profiles after propagation of input Gaussian pulses (10) (dashed line) with initial parameters $P = 0.61$, $\tau = 1.5$ and the pulse at the compression point (solid line) in: the third (a), in fourth core (c), for the 6-core MCF. Graphs (b) and (d) show similar temporal profiles for pulses in 20-th core (b) and 19-th core (d) with initial parameters $P = 0.08035$, $\tau = 3.85$ for the 20-core MCF.

lations. Important to note is that the energy continues to be localized in few cores forming nonstationary light bullets. In terms of practical applications, the input power and the length of the MCF device should be carefully designed to achieve the maximum pulse compression and energy combining.

The increase of the initial modulation depth from 0.03 to 0.3 qualitatively doesn't change the evolution, peak intensity or pulse compression but reduce z_0 to 3.9. The evolution of peak amplitudes and pulse durations in different cores is presented on Fig.3.

A very important point is that compression does not degrade the beam shape. The initial pulse profile and waveform after compression are presented on Fig.4. One can see that small shape deformations are confined to the wings only when the intensity is less then 0.6% of the peak.

The calculation for $N = 20$ with optimizing parameters $P = 0.08035, \tau = 3.85$ results in similar behaviour (see Fig.3). In this case the intensity is lower to suppress the development of small scale perturbations and the peak compression takes place at the longer distance $z_0 = 115.2$. Increasing the number of the cores reduces the pulse width and increases intensity. For a 20-core MCF the pulse width compression factor is around 17.4x, while the peak power in the compressed pulse is increased by 206x. The percentage of the power combined in one core is 72.7%.

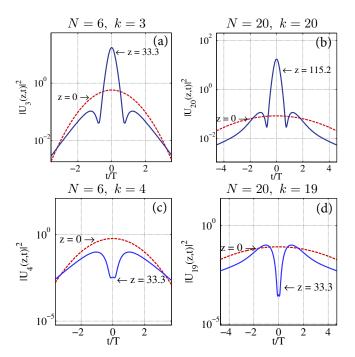Fig. 5 depicts spatial density distribution of the to-

tal power P_t over the cores at the distance of maximum compression for the 6-core and 20-core MCF. For large N, the evolution leading to compression happens at large distance and, in general, we may expect losses to occur during the compression when the power is in excess of P_{cr}. In the asymptotic regime the collapse is easier to arrest and discreteness is more important. One can see that at the peak of compression, the ratio of the peak intensity to the intensity in the neighboring cores is higher for $N = 6$ than for $N = 20$ as seen in Fig. 5.

Thus, we have demonstrated that one can effectively combine the pulse energy in MCFs. This type of nonlinear combining is essentially different from currently popular schemes relying on linear beam combining [17]. When using linear beam combining it is critically important to control the separate beams phases. In our nonlinear combining scheme, the nonlinear interaction self-organizes the process of combining and the phase and pulse shape perturbations at the MCF input are not very important. To demonstrate this feature we consider the evolution of the pulses with random phase variations:

$$\tilde{U}_k = U_k \exp\left[-iC_\delta\right], \ k = 1..N, \tag{11}$$

where $C_\delta = \delta f(k)$ with $f(k)$ being the pseudo-random function with absolute values varying between 0 and 1. More specifically, we model $f(k)$ as $f(k) = \cos(5000k)$.

The modeling demonstrates that the results are not very sensitive to the phase variations. Up to $\delta = 0.8$ the
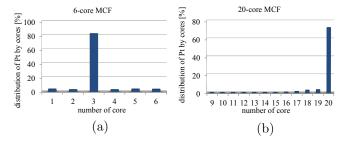
Figure 5. The density distribution of total power P_t over the cores at the distance $z = 33.3$ (a) and $z = 115.2$ (b) - the maximum compression points corresponding to propagation along 6-cores (a) and 20-cores fiber (b) of Gaussian pulses (10).

qualitative picture of the compression doesn't change, the compressed pulse is smooth, the percentage of the power combined into one core doesn't change much, and the compression ratio is almost constant. For example, for $\delta = 0.7$, $N = 20$ the pulse duration compression is about 16.8x, the peak power increases 202.5 times and about 75.6% of all initial power is concentrated into the first core. Notice, that random initial phases lead to a switch of the core where all power is concentrated. More sensitive to the phase fluctuations is the length of compression. For instance, for $\delta = 0$ and $N = 20$ the distance $z_0 = 115.2$, while for $\delta = 0.7$ it is 56.1. In practice, an MCF has some fixed length and phase variations can effect the combining-compression performance. This problem can be fixed in great extent with deeper initial modulation of the intensity distribution in the cores making the system more robust to phase fluctuations. Increasing of the modulation parameter from 0.03 to 0.3 in formula (10) significantly reduces the spread of compression distances at different delta. For example, for a 20-core MCF $z_0 = 28.6$ when $\delta = 0$, and it reaches a minimum $z_0 = 26.1$ at $\delta = 0.5$.

Although our results are general and can be scaled to various system designs, let us make some numerical estimates for typical existing MCFs. Consider $\beta_2 = -20$ ps^2/km and $\gamma = 1.5 \ W^{-1}km^{-1}$. The coupling coefficient parameter varies depending on the particular fiber. For telecom application the coupling must be low and for typical fibers $C = 15.7 \ km^{-1}$ as in [14]. Coming back to the dimensional variable we see that the unit of pulse duration T, $T^2 = -\beta_2/(2C)$, is about 0.8 psec and typical the length $L = 1/C \sim 64 \ m$. It means that our compressor must have a length of a few hundred meters and can compress the pulse up to about 100 femtoseconds. For our nonlinear compressor one can build MCF with more and closer spaced cores and so with a larger coupling coefficient C. If C increases up to $C \sim 1/m$ the length of compressor reduced to the few meters and T is reduced to 0.1 psec and the compressions to pulse durations of ~ 10 femtosecond may be possible, though the model should be modified in this case.

Qualitatively, we anticipate that the ring configuration may be not the optimal scheme for maximum com-

pression. The considered ring design (effectively one-dimensional in k) is equivalent of the 2D system in the continuous limit. Using two-dimensional core distribution designs we will have in a corresponding continuous limit an effective 3D NLSE with strongly collapsing features. It may be more practical to implement the pulses combining and compression in such configurations.

In conclusion, we have examined the pulse combining and compression in a ring MCF configuration. We have demonstrated the effective spatial focusing of energy to only few cores through pre-designed instability of initial spatio-temporal light distribution. Further optimisation of the proposed technique in various MCFs can lead to more efficient pulse compression and pulse combining.

References

1. D. J. Richardson, J. M. Fini, and L. E. Nelson, Nat Photon **7**, 354 (2013).
2. K. Igarashi, T. Tsuritani, and I. Morita, ECOC (2014).
3. A. B. Aceves, G. G. Luther, C. De Angelis, A. M. Rubenchik, and S. K. Turitsyn, Phys. Rev. Lett. **75**, 73 (1995).
4. A. B. Aceves, G. G. Luther, C. De Angelis, A. M. Rubenchik, and S. K. Turitsyn, Optical Fiber Technology **1**, 244 (1995).
5. C. Agger, S. T. Srensen, C. L. Thomsen, S. R. Keiding, and O. Bang, Opt. Lett. **36**, 2596 (2011).
6. S. K. Turitsyn, A. M. Rubenchik, M. P. Fedoruk, and E. Tkachenko, Phys. Rev. A **86**, 031804 (2012).
7. A. M. Rubenchik, E. V. Tkachenko, M. P. Fedoruk, and S. K. Turitsyn, Opt. Lett. **38**, 4232 (2013).
8. S. K. Turitsyn, Phys. Rev. A **47**, R27 (1993).
9. Y. Silberberg, Opt. Lett. **15**, 1282 (1990).
10. S. Minardi, F. Eilenberger, Y. V. Kartashov, A. Szameit, U. Röpke, J. Kobelke, K. Schuster, H. Bartelt, S. Nolte, L. Torner, F. Lederer, A. Tünnermann, and T. Pertsch, Phys. Rev. Lett. **105**, 263901 (2010).
11. T. X. Tran, D. t. . u. C. Duong, and F. Biancalana, Phys. Rev. A **90**, 023857 (2014).
12. Y. S. Kivshar and G. P. Agrawal, *Optical solitons : from fibers to photonic crystals* (Academic, New York, 2003), 5th ed.
13. A. B. Aceves, A. M. Rubenchik, S. K. Turitsyn, and C. De Angelis, Opt. Lett. **19**, 329 (1994).
14. S. Mumtaz, R. Essiambre, and G. Agrawal, Photonics Technology Letters, IEEE **24**, 1574 (2012).
15. G. Agrawal, *Nonlinear Fibre Optics* (Academic Press, Boston, 2013), 4th ed.
16. N. Higham, SIAM J. Matrix Anal. Appl. **26**, 1179 (2005).
17. T. Fan, Selected Topics in Quantum Electronics, IEEE Journal of **11**, 567 (2005).

References

1. D. J. Richardson, J. M. Fini, and L. E. Nelson, "Space-division multiplexing in optical fibres," Nat Photon **7**, 354–362 (2013).

2. K. Igarashi, T. Tsuritani, and I. Morita, "1-exabit/s×km super-nyquist-wdm multi-core-fiber transmission," ECOC (2014).

3. A. B. Aceves, G. G. Luther, C. De Angelis, A. M. Rubenchik, and S. K. Turitsyn, "Energy localization in nonlinear fiber arrays: Collapse-effect compressor," Phys. Rev. Lett. **75**, 73–76 (1995).

4. A. B. Aceves, G. G. Luther, C. De Angelis, A. M. Rubenchik, and S. K. Turitsyn, "Optical pulse compression using fiber arrays," Optical Fiber Technology **1**, 244–246 (1995).

5. C. Agger, S. T. Srensen, C. L. Thomsen, S. R. Keiding, and O. Bang, "Nonlinear soliton matching between optical fibers," Opt. Lett. **36**, 2596–2598 (2011).

6. S. K. Turitsyn, A. M. Rubenchik, M. P. Fedoruk, and E. Tkachenko, "Coherent propagation and energy transfer in low-dimension nonlinear arrays," Phys. Rev. A **86**, 031804 (2012).

7. A. M. Rubenchik, E. V. Tkachenko, M. P. Fedoruk, and S. K. Turitsyn, "Power-controlled phase-matching and instability of cw propagation in multicore optical fibers with a central core," Opt. Lett. **38**, 4232–4235 (2013).

8. S. K. Turitsyn, "Wave collapse and optical-pulse compression," Phys. Rev. A **47**, R27–R29 (1993).

9. Y. Silberberg, "Collapse of optical pulses," Opt. Lett. **15**, 1282–1284 (1990).

10. S. Minardi, F. Eilenberger, Y. V. Kartashov, A. Szameit, U. Röpke, J. Kobelke, K. Schuster, H. Bartelt, S. Nolte, L. Torner, F. Lederer, A. Tünnermann, and T. Pertsch, "Three-dimensional light bullets in arrays of waveguides," Phys. Rev. Lett. **105**, 263901 (2010).

11. T. X. Tran, D. t. . u. C. Duong, and F. Biancalana, "Light bullets in nonlinear waveguide arrays under the influence of dispersion and the raman effect," Phys. Rev. A **90**, 023857 (2014).

12. Y. S. Kivshar and G. P. Agrawal, *Optical solitons : from fibers to photonic crystals* (Academic, New York, 2003), 5th ed.

13. A. B. Aceves, A. M. Rubenchik, S. K. Turitsyn, and C. De Angelis, "Multidimensional solitons in fiber arrays," Opt. Lett. **19**, 329–331 (1994).

14. S. Mumtaz, R. Essiambre, and G. Agrawal, "Reduction of nonlinear penalties due to linear coupling in multicore optical fibers," Photonics Technology Letters, IEEE **24**, 1574–1576 (2012).

15. G. Agrawal, *Nonlinear Fibre Optics* (Academic Press, Boston, 2013), 4th ed.

16. N. Higham, "The scaling and squaring method for the matrix exponential revisited," SIAM J. Matrix Anal. Appl. **26**, 1179–1193 (2005).

17. T. Fan, "Laser beam combining for high-power, high-radiance sources," Selected Topics in Quantum Electronics, IEEE Journal of **11**, 567–577 (2005).